

Supplementary information for
“Energy gaps in $\text{Bi}_2\text{Sr}_2\text{CaCu}_2\text{O}_{8+\delta}$ cuprate superconductors”

J. K. Ren, X. B. Zhu, H. F. Yu, Ye Tian, H. F. Yang, C. Z. Gu, N. L. Wang,
Y. F. Ren and S. P. Zhao*

Beijing National Laboratory for Condensed Matter Physics,
Institute of Physics, Chinese Academy of Sciences, Beijing 100190, China

Supplementary experimental details

Four submicron IJJ mesas (shown schematically in Fig. S1) made of $\text{Bi}_2\text{Sr}_2\text{CaCu}_2\text{O}_{8+\delta}$ crystals with different doping level from underdoped (UD) to overdoped (OD) were used in this work. The labeling of the samples and their parameters are summarized in Table SI. Two samples, UD89K and OD79K, were oxygen doped while the other two yttrium doped. The overdoped OD79K crystals were prepared from the traveling-solvent-floating-zone grown $\text{Bi}_2\text{Sr}_2\text{CaCu}_2\text{O}_{8+\delta}$ crystals by annealing in an oxygen atmosphere. Preparations of the yttrium doped crystals can be found in N. L. Wang, B. Buschinger, C. Geibel, and F. Steglich, Phys. Rev. B54, 7445 (1996).

Details of the mesa fabrication have been described in Refs. [23] and [24]. The mesas were fabricated by lithographically defining the area and removing the surrounding parts by ion milling. Then thin CaF_2 insulating layers were evaporated, and after lift-off, counter electrodes were deposited and defined. For the present spectroscopic study, fabrication of mesas with sizes well below $1\ \mu\text{m}$ was required in order to significantly suppress heating [24]. For this purpose an easier lift-off process was important. In order to achieve this, we have used ZEP520 instead of PMMA950 electron-beam resist to define the mesa area as it is more resistant against Ar-ion milling [Chin. Phys. B19, 087402 (2010)]. Furthermore, the CaF_2 layers should be kept as thin as possible. We found that for our mesas containing typically 10 IJJs, the mesa height was roughly 15 nm and CaF_2 layers with thicknesses as low as 16 to 20 nm could be used.

Since the superconducting transition temperature T_c of the submicron mesas can not be determined directly from the usual temperature dependence of resistance because of their ultra small Josephson critical current, it was thus measured from larger micron-size mesas on the same crystal typically $100\ \mu\text{m}$ away [24]. In Fig. S2, we show the normalized resistance across these mesas versus temperature. T_c was obtained from the sharp drop as temperature decreases. Below it we see in most cases the rising again of the resistance followed by a second but smaller drop at lower temperatures. This feature is attributed to the topmost superconducting layers with slightly reduced T_c due to their contact with the Au films. In rare cases, such feature disappears, as is for the UD80K sample shown in Fig. S2.

I - V curves were measured using 3-terminal configuration shown in Fig. S1. Tunneling spectra (conductance σ) were obtained from numerical differentiation. The conductance peak position (presented as half its value in meV in Fig. 2 with squares) was obtained directly from the measured spectra at lower temperatures. Well above T_c , we first used polynomial fits to the measured spectra

and then determined the peak position from the fitted curves.

The measured tunneling spectra in the entire temperature range are shown in Fig. 1 for the four samples used in this work. In Fig. S3, more detailed data near T_{c0} are presented.

Supplementary figures and table

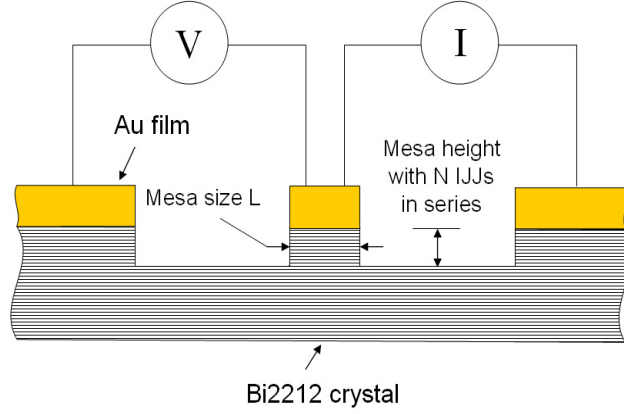


FIG. S1: Schematic mesa-type IJJs and measurement setup.

TABLE SI: Parameters of four mesa-type IJJs fabricated from $\text{Bi}_2\text{Sr}_2\text{CaCu}_2\text{O}_{8+\delta}$ crystals with different doping p ranging from underdoped (UD) to overdoped (OD) levels. L and N are defined in Fig. S1. T_c , T_{c0} and T^* are the superconducting transition temperature, the pair formation temperature and the pseudogap opening temperature, respectively. θ_p is the angle in momentum space, below which the pseudogap phase dominates at higher temperatures (see Fig. 2e). R_N is the normal-state resistance of a single IJJ in a given mesa.

	L^2 (μm^2)	N	T_c (K)	T_{c0} (K)	T^* (K)	p	θ_p ($^\circ$)	R_N (k Ω)
UD71K	0.6×0.6	7	71	150	310	0.10	11	0.4
UD80K	0.3×0.3	9	80	130	280	0.12	10	2.4
UD89K ^a	0.3×0.3	10	89	140	230	0.13	12	1.9
OD79K	0.5×0.5	11	79	100	140	0.21	10	1.4

^aExperimental data published in Eur. Phys. J. B71, 195 (2009).

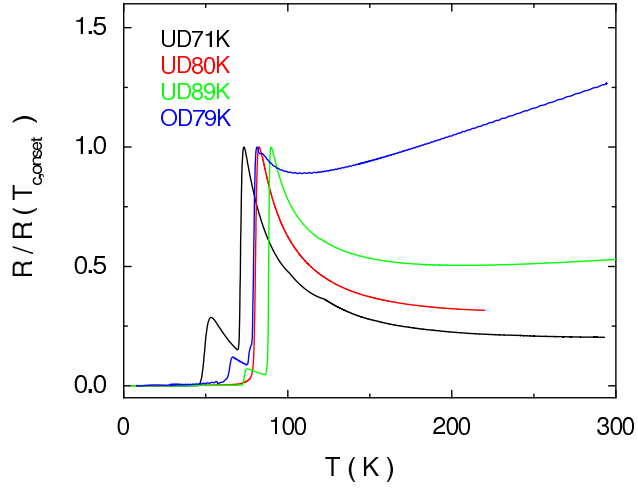


FIG. S2: Temperature dependence of normalized resistance across the mesas which are larger in size and located close to the respective ones in Table SI.

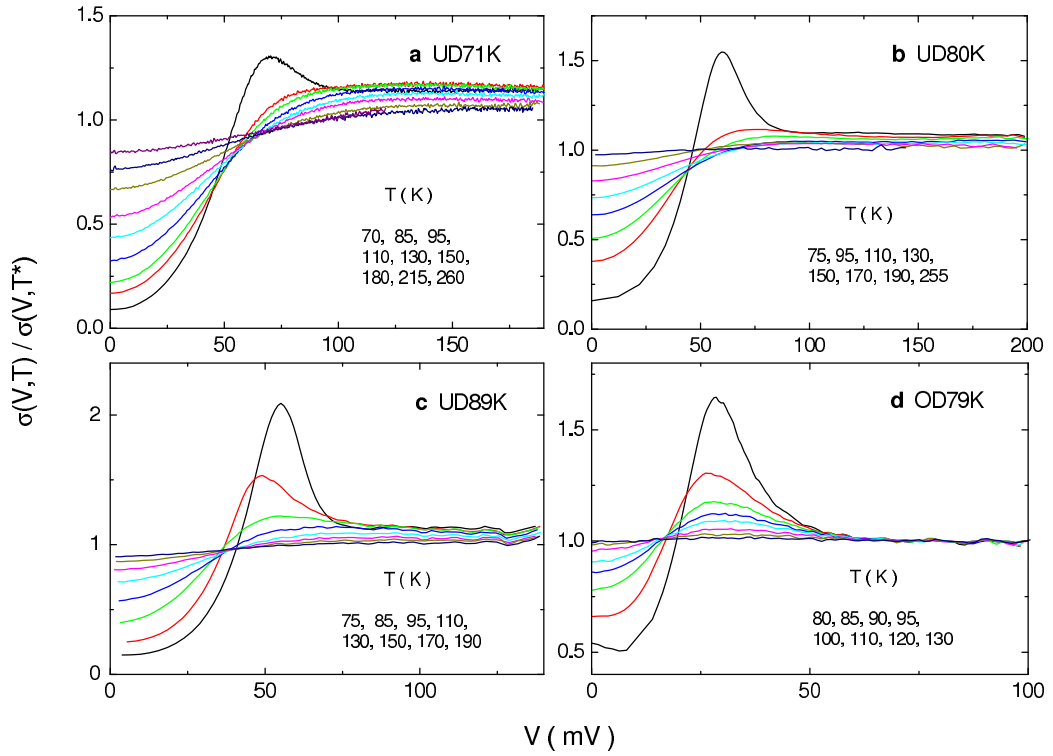


FIG. S3: Experimental tunneling spectra near T_{c0} .

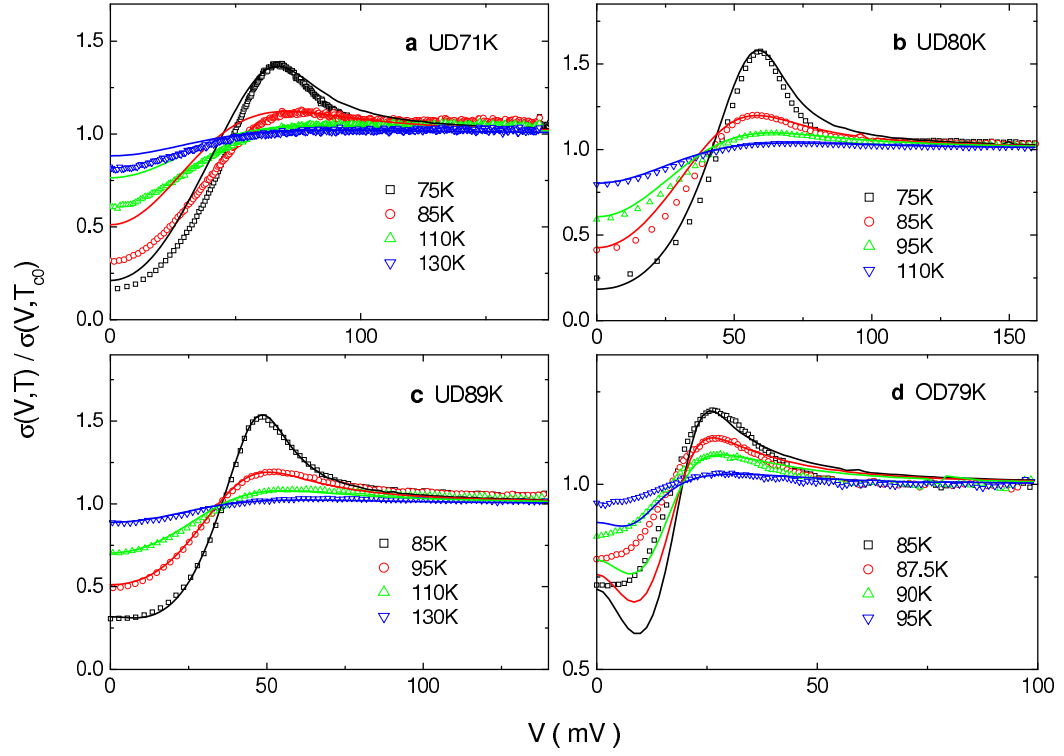


FIG. S4: Experimental (symbols) and calculated (lines) spectra at several temperatures near and above T_c showing the satisfactoriness of the fit for the four samples used in this work. The experimental spectra are normalized to those at T_{c0} . The calculated curves are obtained using equations (1) and (2). The parameters of Δ_s and γ_s in Fig. 2a-d, and θ_p in Table SI are used in the calculations.

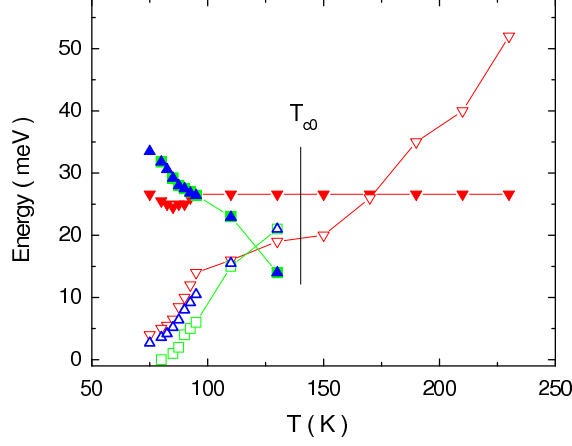


FIG. S5: Comparison of the fitting parameters using two different approaches for the UD89K sample. Up-triangles are Δ_s and γ_s displayed in Fig. 2c and 2f. Down-triangles above T_{c0} are Δ_p and γ_p obtained by fitting the experimental spectra $\sigma(V, T)/\sigma(V, T^*)$ using equation (5) while those below T_{c0} using equation (6) and the Δ_s and γ_s values displayed as up-triangles. Squares show Δ_s and γ_s obtained using equation (6) and the Δ_p and γ_p values at 150 K for temperatures below T_{c0} .

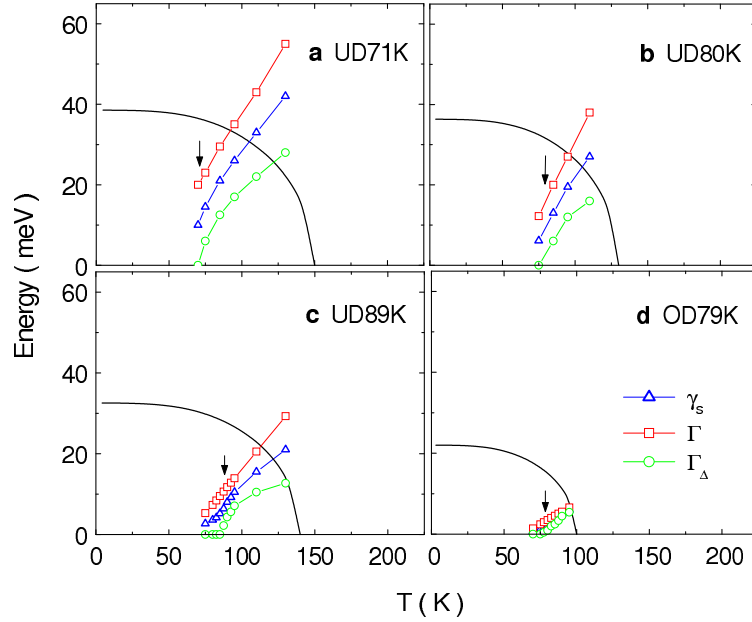


FIG. S6: Temperature dependence of quasiparticle scattering rate Γ and pair decay rate Γ_Δ inferred from experimentally fitted lifetime parameter γ_s in Fig. 2a-d by considering $\gamma_s = (\Gamma + \Gamma_\Delta)/2$ and assuming a linear temperature dependence of Γ ($> \Gamma_\Delta$). Solid lines are BCS gap versus temperature showing the relative size of the data.